Room temperature fabrication of titanium nitride thin films as plasmonic materials by high-power impulse magnetron sputtering

Zih-Ying Yang,[1] Yi-Hsun Chen,[1] Bo-Huei Liao,[2] and Kuo-Ping Chen[3,*]

[1] *Institute of Lighting and Energy Photonics, National Chiao Tung University, 301 Gaofa 3rd Road, Tainan 711, Taiwan*

[2] *Instrument Technology Research Center, National Applied Research Laboratories, Hsinchu 300, Taiwan*

[3] *Institute of Imaging and Biomedical Photonics, National Chiao Tung University, 301 Gaofa 3rd Road, Tainan 711, Taiwan*

[*] *kpchen@nctu.edu.tw*

Abstract: High-power impulse magnetron sputtering (HiPIMS) was used to deposit titanium nitride (TiN) thin films with high electron density as alternative plasmonic materials. TiN thin films with thicknesses of 20–40 nm were deposited with different average sputtering powers, and exhibited metallic- and dielectric-like optical properties. When the sputtering power was increased from 80 W to 300 W, denser polycrystalline TiN thin films were obtained at room temperature (RT) with a conductivity 25 times that of the low-sputtering-power film. With sufficient average power (≥ 180 W), the films exhibited metallic-like optical properties, and a conductivity of >10^5 S/m. By using HiPIMS deposition, good-quality metallic-like TiN thin films could be fabricated at RT without heating the substrate.

©2016 Optical Society of America

OCIS codes: (250.5403) Plasmonics; (310.0310) Thin films.

References and links

1. P. R. West, S. Ishii, G. V. Naik, N. K. Emani, V. M. Shalaev, and A. Boltasseva, "Searching for better plasmonic materials," Laser Photonics Rev. **4**(6), 795–808 (2010).
2. J. B. Khurgin and A. Boltasseva, "Reflecting upon the losses in plasmonics and metamaterials," MRS Bull. **37**(08), 768–779 (2012).
3. A. Boltasseva and H. A. Atwater, "Materials science. Low-loss plasmonic metamaterials," Science **331**(6015), 290–291 (2011).
4. G. V. Naik, J. L. Schroeder, X. Ni, A. V. Kildishev, T. D. Sands, and A. Boltasseva, "Titanium nitride as a plasmonic material for visible and near-infrared wavelengths," Opt. Mater. Express **2**(4), 478–489 (2012).
5. V. E. Babicheva, N. Kinsey, G. V. Naik, M. Ferrera, A. V. Lavrinenko, V. M. Shalaev, and A. Boltasseva, "Towards CMOS-compatible nanophotonics: Ultra-compact modulators using alternative plasmonic materials," Opt. Express **21**(22), 27326–27337 (2013).
6. A. Anders, "A review comparing cathodic arcs and high power impulse magnetron sputtering (HiPIMS)," Surf. Coat. Tech. **257**, 308–325 (2014).
7. F. Magnus, A. S. Ingason, O. Sveinsson, S. Olafsson, and J. Gudmundsson, "Morphology of TiN thin films grown on SiO_2 by reactive high power impulse magnetron sputtering," Thin Solid Films **520**(5), 1621–1624 (2011).
8. C.-L. Chang, S.-G. Shih, P.-H. Chen, W.-C. Chen, C.-T. Ho, and W.-Y. Wu, "Effect of duty cycles on the deposition and characteristics of high power impulse magnetron sputtering deposited TiN thin films," Surf. Coat. Tech. **259**, 232–237 (2014).
9. Y. Igasaki and H. Mitsuhashi, "The effects of substrate bias on the structural and electrical properties of TiN films prepared by reactive rf sputtering," Thin Solid Films **70**(1), 17–25 (1980).
10. G. Janssen and J.-D. Kamminga, "Stress in hard metal films," Appl. Phys. Lett. **85**(15), 3086–3088 (2004).
11. F. Magnus, A. S. Ingason, S. Olafsson, and J. T. Gudmundsson, "Nucleation and Resistivity of Ultrathin TiN Films Grown by High-Power Impulse Magnetron Sputtering," IEEE Electron Device Lett. **33**(7), 1045–1047 (2012).
12. K. A. Aissa, A. Achour, J. Camus, L. Le Brizoual, P.-Y. Jouan, and M.-A. Djouadi, "Comparison of the structural properties and residual stress of AlN films deposited by dc magnetron sputtering and high power impulse magnetron sputtering at different working pressures," Thin Solid Films **550**, 264–267 (2014).
13. J. Lin, J. J. Moore, W. D. Sproul, B. Mishra, Z. Wu, and J. Wang, "The structure and properties of chromium nitride coatings deposited using dc, pulsed dc and modulated pulse power magnetron sputtering," Surf. Coat. Tech. **204**(14), 2230–2239 (2010).

#245651 Received 14 Jul 2015; revised 14 Dec 2015; accepted 14 Jan 2016; published 20 Jan 2016

14. M. Samuelsson, D. Lundin, J. Jensen, M. A. Raadu, J. T. Gudmundsson, and U. Helmersson, “On the film density using high power impulse magnetron sputtering,” Surf. Coat. Tech. **205**(2), 591–596 (2010).
15. U. Guler, G. V. Naik, A. Boltasseva, V. M. Shalaev, and A. V. Kildishev, “Performance analysis of nitride alternative plasmonic materials for localized surface plasmon applications,” Appl. Phys. B **107**(2), 285–291 (2012).
16. M. Aiempanakit, A. Aijaz, D. Lundin, U. Helmersson, and T. Kubart, “Understanding the discharge current behavior in reactive high power impulse magnetron sputtering of oxides,” J. Appl. Phys. **113**(13), 133302 (2013).
17. S. Konstantinidis, J. Dauchot, and M. Hecq, “Titanium oxide thin films deposited by high-power impulse magnetron sputtering,” Thin Solid Films **515**(3), 1182–1186 (2006).
18. J.-H. Huang, F.-Y. Ouyang, and G.-P. Yu, “Effect of film thickness and Ti interlayer on the structure and properties of nanocrystalline TiN thin films on AISI D2 steel,” Surf. Coat. Tech. **201**(16-17), 7043–7053 (2007).
19. K. Sarakinos, J. Alami, and S. Konstantinidis, “High power pulsed magnetron sputtering: A review on scientific and engineering state of the art,” Surf. Coat. Tech. **204**(11), 1661–1684 (2010).
20. S. Logothetidis, E. Meletis, and G. Kourouklis, “New approach in the monitoring and characterization of titanium nitride thin films,” J. Mater. Res. **14**(02), 436–441 (1999).
21. J. H. Kang and K. J. Kim, “Structural, optical, and electronic properties of cubic TiNx compounds,” J. Appl. Phys. **86**(1), 346–350 (1999).
22. G. V. Naik, J. Kim, and A. Boltasseva, “Oxides and nitrides as alternative plasmonic materials in the optical range [Invited],” Opt. Mater. Express **1**(6), 1090–1099 (2011).
23. M. Lattemann, U. Helmersson, and J. Greene, “Fully dense, non-faceted 111-textured high power impulse magnetron sputtering TiN films grown in the absence of substrate heating and bias,” Thin Solid Films **518**(21), 5978–5980 (2010).
24. H. T. Kim, J. Y. Park, and C. Park, “Effects of nitrogen flow rate on titanium nitride films deposition by DC facing target sputtering method,” Korean J. Chem. Eng. **29**(5), 676–679 (2012).
25. H. Guo, T. P. Meyrath, T. Zentgraf, N. Liu, L. Fu, H. Schweizer, and H. Giessen, “Optical resonances of bowtie slot antennas and their geometry and material dependence,” Opt. Express **16**(11), 7756–7766 (2008).
26. S. Prayakarao, S. Robbins, N. Kinsey, A. Boltasseva, V. Shalaev, U. Wiesner, C. Bonner, R. Hussain, N. Noginova, and M. Noginov, “Gyroidal titanium nitride as nonmetallic metamaterial,” Opt. Mater. Express **5**(6), 1316–1322 (2015).
27. R. Bavadi and S. Valedbagi, “Physical properties of titanium nitride thin film prepared by DC magnetron sputtering,” Mater. Phys. Mech. **15**, 167–172 (2012).
28. K.-P. Chen, V. P. Drachev, J. D. Borneman, A. V. Kildishev, and V. M. Shalaev, “Drude relaxation rate in grained gold nanoantennas,” Nano Lett. **10**(3), 916–922 (2010).
29. R. Machunze, A. Ehiasarian, F. Tichelaar, and G. Janssen, “Stress and texture in HIPIMS TiN thin films,” Thin Solid Films **518**(5), 1561–1565 (2009).
30. M. Benegra, D. Lamas, M. F. De Rapp, N. Mingolo, A. Kunrath, and R. Souza, “Residual stresses in titanium nitride thin films deposited by direct current and pulsed direct current unbalanced magnetron sputtering,” Thin Solid Films **494**(1-2), 146–150 (2006).

1. Introduction

For plasmonic applications, traditional noble metals have a high loss problem, which affects the surface plasmon coupling excitation between photons and free-electrons [1]. To create better plasmonic materials, the high losses should be reduced in order to ensure plasmon resonance enhancement efficiency. According to the literature, methods have been proposed to reduce the losses, such as adding a gain medium or using new intermediate carrier density materials with tunable band structures [2]. There are two important parameters that determine the conductivity of materials: carrier concentration and carrier mobility. The carrier concentration determines the plasma frequency, while the carrier mobility reflects losses in the material. In addition, losses also result from interband transitions between the conduction and valence bands [3]. To achieve a low-loss plasmonic material using semiconductor, which possess tunable properties, large bandgap is required that reduces interband transition losses and also high plasma frequency is needed to attain a negative real permittivity at the intended optical frequency [2]. According to the literature, transition metal nitrides exhibit metallic behavior in the visible and near-IR ranges and have been proposed as a promising alternative plasmonic material [4]. There are also additional advantages of transition metal nitrides such as chemical stability, high melting temperature, and tunable optical properties. Hence, these low-loss plasmonic materials have recently received a lot of attention. Since transition metal nitrides possess a high melting point, it is difficult to evaporate or sputter directly from a nitride source. One common method for nitride deposition is magnetron sputtering with a reaction between nitrogen gas and the metal target [5].

#245651 Received 14 Jul 2015; revised 14 Dec 2015; accepted 14 Jan 2016; published 20 Jan 2016
© 2016 OSA

There are several types of reactive sputtering sources, direct current (DC), radiofrequency (RF), and high-power impulse magnetron sputtering (HiPIMS) [6]. In the past, DC sputtering was the most simple and common technology. However, the fast development of HiPIMS has gathered a lot of attention lately because of its higher ionization among all magnetron sputtering processes and the ease of connecting a HiPIMS setup to a DC power supply [7]. Due to the high-power input of a short pulse to the target, the high plasma density (10^{17} to 10^{19} m^{-3}) is several orders of magnitude higher than that of conventional DC sputtering (10^{14} to 10^{16} m^{-3}) [8]. There is also another simple way to increase the plasma density by increasing the substrate bias voltage [9]. However, the lattice defects could be resulted from the relatively high bias voltages [10]. Magnetron sputtering with the HiPIMS technique is an advanced sputtering technique wherein the pulse of power applied to the target has a low duty cycle (or on/off time ratio) that is less than 10% and a pulse time of less than one hundred microseconds [11]. Although the longer pulse off-time reduces the deposition rate and the excessive ion bombardment energy might cause stress, this technique has the advantage in generating ultra-dense plasmas with a high concentration of ionized sputtered atoms [12]. Therefore, HiPIMS could not only optimize the performance of compound deposited films, but also make the films denser due to the effective momentum transfer, which results in the less pores thin films deposition [13, 14].

In literatures, by controlling temperature, substrate, or the deposition gas ratio, TiN could reach low loss in visible and NIR wavelengths, while the optical properties can also be adjusted [15]. However, there has been less discussion on using the HiPIMS to fabricate the metallic-like and dielectric-like TiN thin films. Compared to conventional magnetron sputtering, HiPIMS could provide a higher degree of ionization of the sputtered metal and a higher rate of molecular gas dissociation [16]. Because the increasing ionization rate leads to more energetic ions and enables better reaction during the growth of the film, the sputtered films by using HiPIMS technique could be more condensation and possess higher refractive index [17]. However, most of the published works using HiPIMS discuss fabrication of thicker TiN films to harden and protect cutting and sliding surfaces or studying electrical property, but less research discusses thin TiN or its optical properties [18]. In this study, the improvement in density of TiN thin films by HiPIMS at a lower deposition temperature is achieved. The effects of the average power parameter and thickness on the conductivity, crystallinity, and optical resonant properties of the TiN thin film are investigated. Finally, the relationships between electrical and optical properties of the TiN thin films are shown.

2. Titanium nitride thin-film fabrication

In the deposition system, Ar-Ti HiPIMS discharge operates at a pulse on/off time of 45/955 μs. During the pulse-on time, there is a constant voltage but a significantly increased peak target current. For conventional direct current magnetron sputtering, the plasma power density is not high enough for a high degree of ionization as it is on the order of only 10^{14} to 10^{16} m^{-3} [6]. One way to increase the power density, and also avoid the target melting problem, is to use short pulses that operate under low average power but possesses high power during the pulse-on time [19]. Therefore, the optical properties of TiN thin films with different average power density processes under HiPIMS are of interest to investigate.

TiN thin films were deposited on B270 glass substrates by reactive HiPIMS (SPIK 2000A). The deposition chamber was pumped down to 5×10^{-6} Torr. The titanium sputtering targets were 99.99% pure discs (100 mm in diameter). The sputtering process began at a pressure of 2.2 mTorr. An average power supply of 300 W was used in this experiment. The flow rate of argon was fixed at 30 sccm, and the flow rate of reactive nitrogen was 3 sccm. Figure 1(a) shows a 3D AFM image of a TiN thin film with the measured root mean square roughness (R_q) around 1.6 nm. A SEM image of a TiN thin film shows the thickness of the films is around 45 nm with smooth surface. In order to investigate the effect of HiPIMS on properties of the TiN thin films, the average power was fixed and the power density increased

#245651 Received 14 Jul 2015; revised 14 Dec 2015; accepted 14 Jan 2016; published 20 Jan 2016
© 2016 OSA

to 2 and 20 times the initial power density by adjusting the pulse on/off ratio (45/45 μs and 45/955 μs).

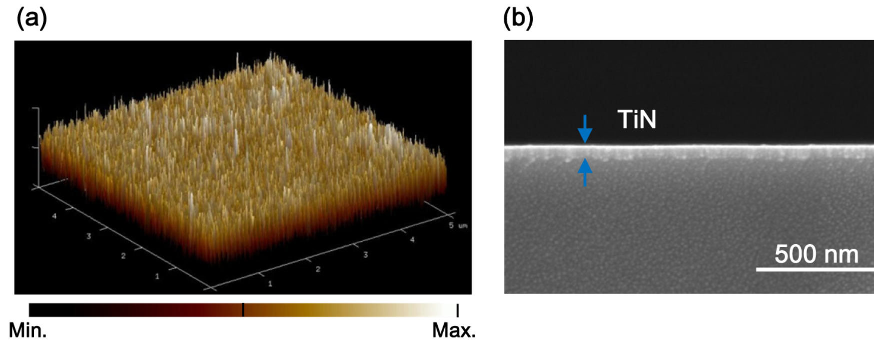

Fig. 1. A 45-nm TiN thin film deposited with an average power of 300 W, HiPIMS on/off ratio equal to 45 μs /955 μs, and 400 °C heating process. (a) AFM image (b) Cross-section SEM image.

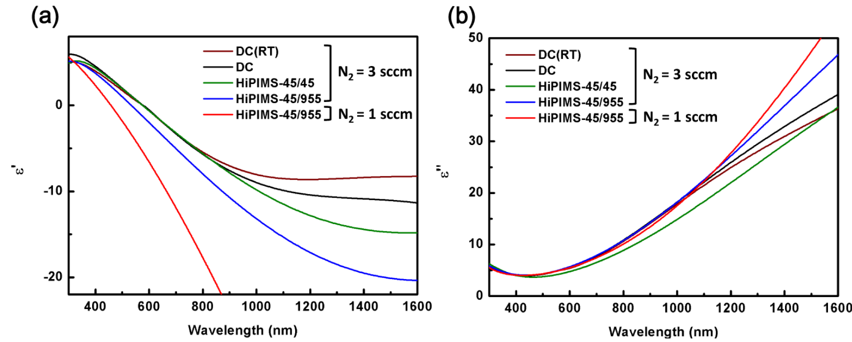

Fig. 2. The (a) real part and (b) imaginary part of the dielectric functions of TiN thin films deposited by traditional DC sputtering (black), HiPIMS with an on/off ratio equal to 45 μs /45 μs (green), and HiPIMS with an on/off ratio equals to 45 μs /955 μs (blue). The average power is 300 W with a 400 °C heating process. The 40-nm TiN film deposited by HiPIMS with an on/off ratio of 45 μs /955 μs has a larger negative real and imaginary permittivity than the HiPIMS-45/45, and exhibits more metallic-like behavior. Compared to the DC sample, the HiPIMS-45/955 sample possesses a similar imaginary permittivity but exhibits stronger metallic properties. The TiN thin films deposited at RT using DC magnetron sputtering (brown) and at 400°C using HiPIMS with lower nitrogen flow (N_2 = 1sccm, red) were also shown.

The TiN film thickness and refractive index were characterized by spectroscopic ellipsometry (M-2000, J. A. Wollam Co.). The refractive index of TiN thin films is fitted by the Drude and Lorentz models at wavelengths ranging from 190 to 1700 nm. Figure 2 shows the dielectric function for the HiPIMS pulse on/off ratios of 45/955, 45/45, and the DC samples. As shown in Fig. 2(a), all of the samples have a negative value of the real part of the dielectric function and exhibit metallic behavior in the visible/near-infrared wavelength range. With HiPIMS, by using flow rate of reactive nitrogen as low as 1 sccm, the thin film could reach stoichiometric TiN_x (x ~1). Increasing nitrogen flow rates, TiN_x becomes overstoichiometric (x > 1) and shows the upward trend of the real permittivity at longer wavelengths. In this work, the overstoichiometric samples are mainly focused because it will be benefit to study the HiPIMS power effect. When comparing the samples using DC sputtering with different temperatures, the thin film deposited at 400°C could get a more negative value of real permittivity. In addition, when using the HiPIMS operating at 45/45 and 45/955 could also lead to a further increase to negative value of real permittivity. High temperature process is generally utilized to reduce the structural defects and resulting in better

#245651 Received 14 Jul 2015; revised 14 Dec 2015; accepted 14 Jan 2016; published 20 Jan 2016
© 2016 OSA

reaction during the thin films growth. Hence, it can be inferred that using HiPIMS operating at low duty cycle (4.5% for HiPIMS 45/955) could fabricate highly metallic-like properties thin films. Figure 2(b) shows the imaginary part of the dielectric function. Compared to the DC sample, the slightly higher bombardment energy (HiPIMS 45/45) sample possesses a smaller value of the imaginary part, which shows lower loss. For Drude-like metals, the losses at longer wavelengths are mainly caused by free electron losses [1]. The losses scale up directly with carrier concentration. Because of the higher cross-over frequency comparing to the

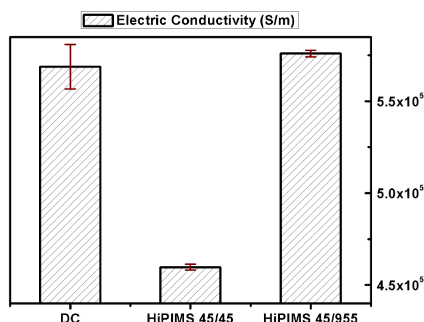

Fig. 3. Derived conductivity of TiN thin films deposited by traditional DC sputtering, HiPIMS using an on/off ratio equal to 45 μs /45 μs, and HiPIMS using an on/off ratio equal to 45 μs /955 μs. In Fig. 3, the HiPIMS-45/955 sample has a slightly higher conductivity compared to that of the DC sample, but with a much smaller measurement deviation. The HiPIMS-45/955 sample exhibits an obvious improvement in conductivity as compared to the HiPIMS-45/45 sample.

HiPIMS 45/45 sample, HiPIMS 45/955 sample has higher concentration of free carriers, so there would be higher losses.

Figure 3 shows the derived electric conductivity using four-point probe measurement. When the power density is decreased, the decrease of the conductivity may be due to more electrons being scattered by nitrogen molecules [19]. For example, the conductivity decreases as the power density (HiPIMS 45/955) decreases to a lower value (HiPIMS 45/45). The HiPIMS 45/955 sample possesses the best conductivity compared to the other two samples. Because the samples in Fig. 3 are overstoichiometric, comparing to DC sputtering, under HiPIMS deposition there would be better reaction result from more energetic ions, which could lead to a higher N/Ti ratio with lower carrier concentration. Therefore, the DC sample is with higher conductivity than HiPIMS 45/45 sample [20, 21]. By shortening the duty cycle, HiPIMS 45/955 sample is with higher carrier mobility resulting from the denser film comparing to HiPIMS 45/45 sample [14]. Therefore, the conductivity of HiPIMS 45/955 sample is improved. Furthermore, the deviation of the derived conductivity in the HiPIMS 45/955 sample is relatively smaller than that of the DC sample, which means the quality of samples under the HiPIMS process is more uniform. Hence, in the following experiment, TiN films deposited by HiPIMS operating under a 45/955 pulse on/off time ratio are chosen.

In general, heating during thin-film deposition promotes electrical conductivity [7]. Regardless of deposition at RT or up to 600 °C, the HiPIMS samples have lower resistivity than the DC samples [11]. In the literature, the film thickness is also an important factor that modifies the optical properties of alternative plasmonic thin films, especially when the thickness is less than 50 nm [22]. There are two ways could effectively enhance the plasma density (the degree of ionization of the plasma particles); one is adding bias voltage to the substrate, while the other is using HiPIMS technique [19]. In DC sputtering, increasing the power usually cannot change the film quality. However, HiPIMS deposition is strongly depended on power density because the instantaneous power of HiPIMS could easily reach several MW [20, 23]. Therefore, in this study, the discussion focuses on tuning the sputtering average power with HiPIMS technique in both RT and 400 °C heating processes. In addition,

#245651 Received 14 Jul 2015; revised 14 Dec 2015; accepted 14 Jan 2016; published 20 Jan 2016
© 2016 OSA

Table 1. Magnetron sputtering with HiPIMS technique process parameters for TiN thin-film deposition.

Sample No.	Temperature: 400 °C		Sample No.	Temperature: RT		Sample No.	Temperature: RT	
	Power (W)	Thickness (nm)		Power (W)	Thickness (nm)		Power (W)	Thickness (nm)
S1	300	45	S4	300	48	S7	300	23
S2	180	45	S5	180	48	S8	180	23
S3	80	45	S6	80	48	S9	80	23

the thickness effects are discussed. Three sputtering powers were chosen: 300 W, 180 W, and 80 W, as shown in Table 1. The Group 1 samples (S1, S2, and S3) have a 400 °C deposition temperature and a thickness of 45 nm (the thickness deviation is 2 nm). The Group 2 samples (S4, S5, and S6) were deposited at RT and have thicknesses similar to those in Group 1 (48 nm with a 2 nm deviation in thickness). The Group 3 samples (S7, S8, and S9) were deposited at RT and have thicknesses of 23 nm (the thickness deviation is 1 nm). The time averaged deposition rate ranges from 0.6 Å/s to 0.2 Å/s when the sputtering power was decreased from 300 W to 80 W.

3. Characterization of optical, electrical, and crystalline properties

Although some researchers have investigated the effects of process power density on TiN thin-film properties [20], there has been less emphasis on how to separate the metallic-like and dielectric-like TiN thin films that are formed when the power density is adjusted. In this study, the flow rate of argon is fixed at 30 sccm and the flow rate of reactive nitrogen is 3 sccm. The on/off time ratio of HiPIMS was fixed at 45/955 μs. By tuning the sputtering time average power, two sets of TiN thin films could be fabricated. One has a negative real part of permittivity (metallic-like), while the other has a positive real permittivity at all visible and NIR wavelengths (dielectric-like). Further discussions on the relations between the optical and electrical properties, along with the crystalline properties, are shown in the next section.

3.1 Optical properties of TiN thin films

Figure 4 shows the dielectric function of the TiN thin films fabricated under different average power. Compared to the samples with RT deposition (Group 2: S4, S5 and S6 indicated by the green line and solid symbol), the samples deposited at 400 °C have a higher plasma frequency (Group 1: S1, S2 and S3 indicated by the black line with solid symbol). Interestingly, the thinner samples (Group 3: S7, S8 and S9 indicated by the blue line with hollow symbol) under RT deposition have a plasma frequency similar to that of the samples in Group 1.

Clearly, when the average power is increasing from 80 W to 300 W, the ellipsometry results show that the dielectric function will change from dielectric-type to conductor-type. The reason for this change is that the reduced power would lead to the bombardment of fewer titanium particles resulting in a more efficient reaction with nitrogen. Hence, the TiN thin films deposited at lower power present dielectric characteristics. Samples having a negative real permittivity can be seen as metallic-like samples and samples with positive real permittivity in the optical regions are regarded as dielectric-like samples (S3, S6, and S9). According to literatures, metal-rich TiN thin films could also be deposited by adjusting the flow rate of the nitrogen gas [24]. However, with higher power HiPIMS process, the stronger effective momentum transfer process during the growth of the film could fabricate not only metal-rich but also significantly lower resistivity TiN thin films [11].

The Drude-Lorentz model can be used to model the dielectric function of TiN thin films, that single term Lorentz is considered, as shown in Eq. 1.1 to Eq. 1.3 [5, 25, 26]

$$\varepsilon = \varepsilon_1 + i\varepsilon_2 = \varepsilon_b - \frac{\omega_P^2}{\omega^2 + i\gamma_D\omega} + \frac{f}{\omega_0^2 - \omega^2 - i\gamma_L\omega} \tag{1.1}$$

#245651 Received 14 Jul 2015; revised 14 Dec 2015; accepted 14 Jan 2016; published 20 Jan 2016
© 2016 OSA

$$\omega_P^2 = \frac{\sigma_0}{\varepsilon_0 \tau} = \frac{\sigma_0 \gamma_D}{\varepsilon_0} = \frac{ne^2}{\varepsilon_0 m}, \text{ where } \sigma_0 = \frac{ne^2 \tau}{m} \tag{1.2}$$

$$\rho_0 = \frac{1}{\sigma_0} = \frac{\gamma_D}{\varepsilon_0 {\omega_p}^2} \tag{1.3}$$

where ε_b, ω_P, γ_D, σ_0, ρ_0, $\tau = 1/\gamma_D$, m, e and ε_0 are the background permittivity, plasma frequency, damping frequency, conductivity, resistivity, relaxation time, electron mass, electron charge, and vacuum permittivity, respectively. (f, γ_L) are (Lorentz oscillator strength and oscillator damping rate), and ω_0 is the natural frequency of the oscillation.

In plasmonic materials, the conductivity plays an important role such that metal materials with higher conductivity have a higher electron density (n) and longer electron relaxation time (τ). In Table 2, the frequency dependent dielectric functions of the metallic samples are fitted by the Drude model.

A commercial spectroscopy system (U4100, HITACHI) is used to measure the reflectance and transmittance spectra of the TiN thin films at wavelengths ranging from 240 nm to 1600 nm. In order to verify the dielectric constant fitted by ellipsometry, the experimental results were compared with the calculated spectra by using the dielectric constant derived from ellipsometry measurements. In Fig. 5, the modeling spectra fit well with the experimental results. The sample possessing the higher plasma frequency accompanies a higher carrier concentration and the resonance wavelength is blue-shifted. The wavelengths of the reflectance dips for each sample are 580 nm (S3), 490 nm (S2), and 438 nm (S1), as shown in Fig. 5(a). The wavelengths of the transmittance peaks are 522 nm (S3), 491 nm (S2), and 458 nm (S1), as shown in Fig. 5(b). When the average power is higher, there are not only more titanium atoms ejected but also with better reaction with nitrogen, which results in denser film deposition [19]. A denser film can be regarded as a high quality film, which contains a higher carrier concentration per unit volume. The corresponding resonance wavelength will appear at a shorter wavelength, which shows good agreement with the results in the literature [22].

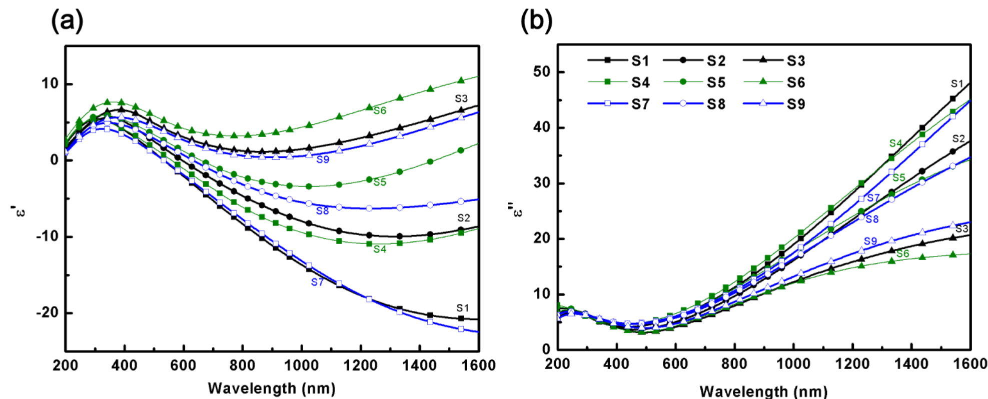

Fig. 4. (a) Real and (b) imaginary part of the dielectric function for TiN thin films under the different deposition parameters illustrated in Table 1. Group 1 (deposition at 400 °C with a thickness of 45 nm) is indicated by the black line with solid symbol, with three different average powers: 300 W, 180 W, and 80 W for S1, S2, and S3. Group 2 (deposition at room temperature with a thickness of 48 nm) is indicated by the green line with solid symbol. Group 3 (room temperature process with a thickness of 23 nm) is indicated by the blue line with hollow symbol. When the average power is greater than 180 W, the TiN samples exhibit metallic-like dielectric functions regardless of the thin-film thickness and deposition temperature.

#245651 Received 14 Jul 2015; revised 14 Dec 2015; accepted 14 Jan 2016; published 20 Jan 2016
© 2016 OSA

Table 2. Plasma frequencies of metallic-like TiN thin films.

Sample No.	Temperature: 400 °C ω_p (x2π THz)		Temperature: RT ω_p (x2π THz)		Temperature: RT ω_p (x2π THz)
S1	1862	S4	1846	S7	1846
S2	1767	S5	1511	S8	1623

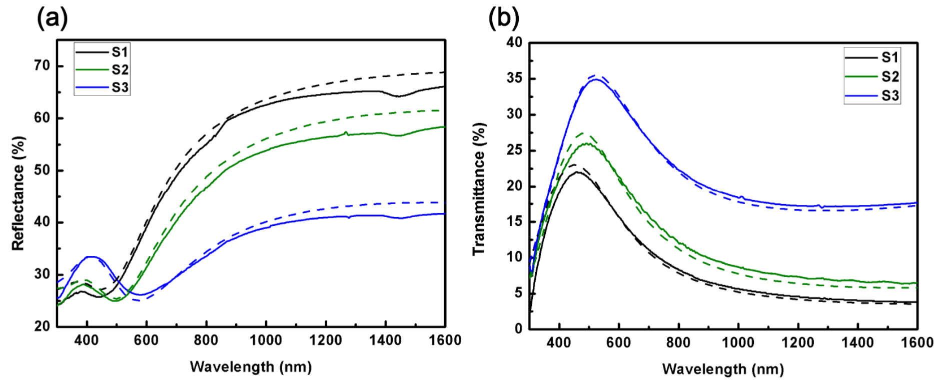

Fig. 5. (a) Reflectance and (b) transmittance spectra for TiN thin films for Group 1 samples deposition at 400 °C with a thickness of 45 nm). The average power is 300 W for S1 (black), 180 W for S2 (green), and 80 W for S3 (blue). The experimental reflectance and transmittance spectra are indicated by a solid line; the modeling reflectance and transmittance spectra are indicated by a dashed line.

3.2 Electrical properties of TiN thin films

Figure 6 shows the four-point probe measurement results of all samples. For all samples, the conductivity increases as the average power increases. In addition, when deposition at 400 °C, all samples (black line – S1, S2, S3; and brown line – S10, S11, S12) possess higher conductivity than samples deposited at RT with same thickness. The conductivity is around 2.59×10^4 S/m to 7.65×10^5 S/m.

3.3 Crystalline properties of TiN thin films

The crystalline properties of the TiN thin films are measured by grazing incidence X-ray diffraction (D5000, SIEMENS). The XRD measurement results shown in Fig. 7 were attained using grazing incidence at θ = 1° with an angular resolution of 0.1°. The obvious (111), (200), and (220) crystal orientation peaks are present in the most metallic-like sample (S1). This means that the higher average power results in a more polycrystalline TiN film. The main peak is at (200), that 2θ = 42.4° – 42.55° with a small shift. The Debye-Scherrer's formula was used to estimate the the grain size in (200) phase [27, 28]

$$d = \frac{0.9\lambda}{\beta \cos\theta} \tag{2}$$

where λ is X-ray wavelength (for Cu(Kα) = 0.154 nm), θ is the Bragg angle, and β is full width at half maximum (FWHM) intensity of the sample.

#245651 Received 14 Jul 2015; revised 14 Dec 2015; accepted 14 Jan 2016; published 20 Jan 2016
© 2016 OSA

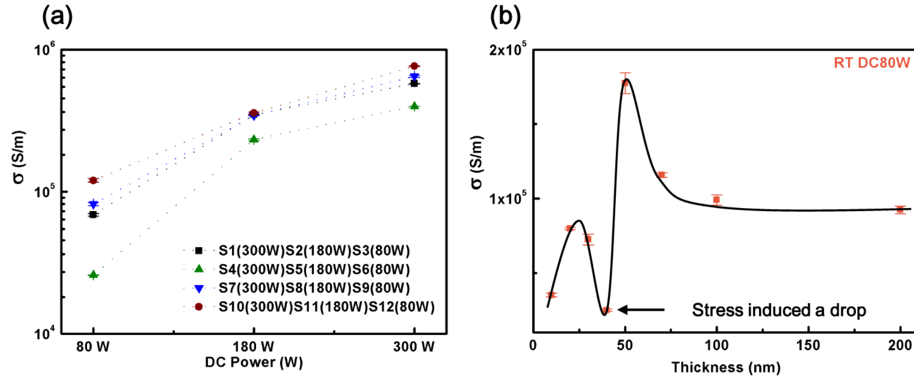

Fig. 6. (a) Derived conductivity (σ) for TiN thin films with the deposition parameters from Table 1. Group 1 (400 °C heating process with a thickness of 45 nm for S1, S2, and S3) is indicated by the black line. Group 2 (room temperature process with a thickness of 48 nm for S4, S5, and S6) is indicated by the green line. Group 3 (room temperature process with a thickness of 23 nm, for S7, S8, and S9) is indicated by the blue line. In addition, 400 °C heating process with a thickness of 22 nm for (S10, S11, and S12) is indicated by the brown line. (b) Conductivity shows thickness-dependent properties (< 50 nm) due to the variation of the stress during the growth of the films. The solid square represents the experimental results.

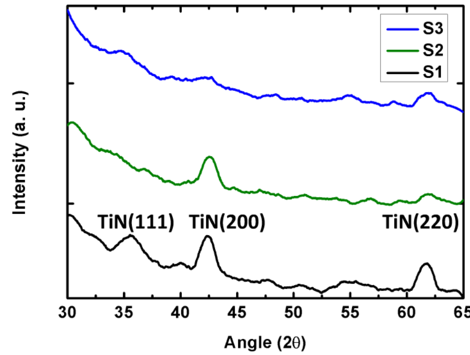

Fig. 7. XRD measurement for Group 1 samples (deposition at 400 °C with a thickness of 45 nm). Samples S1 (300 W), S2 (180 W) and S3 (80 W) show difference in diffraction peaks. There are three peak orientations visible: (111), (200) and (220). S1 shows the largest diffraction signals comparing to S2 and S3.

4. Discussion

4.1 Optical properties and Drude model fitting parameters

As Fig. 4 indicates, the deposition power of HiPIMS must be larger than a certain value (≥ 180 W) to fabricate a metallic-like TiN thin film. Compared to the samples subjected to a change in thickness or deposition temperature, the samples deposited using a higher power density are accompanied by a more negative real part and a larger imaginary part of the permittivity. As listed in Table 2, when the sample is deposited at a higher average power, it has a higher plasma frequency (S1 > S2, S4 > S5, and S7 > S8). The sample would also have a higher carrier concentration (Eq. 1.2). Under high power HiPIMS deposition, the sample deposited at a higher temperature could only experience a slight increase of the plasma frequency, which means that while using high power HiPIMS deposition, good quality metallic-like TiN thin films could be fabricated at RT. RT deposition could be very helpful and convenient for samples with soft substrates or with photoresist. When deposition power increases, a high quality film, which contains a higher carrier concentration, could be fabricated such that the negative real permittivity would appear at a shorter wavelength. This

#245651 Received 14 Jul 2015; revised 14 Dec 2015; accepted 14 Jan 2016; published 20 Jan 2016
© 2016 OSA

permittivity is accompanied by a higher plasma frequency that results in blue-shifted resonance wavelengths.

4.2 Electrical properties and crystalline properties

Under high power HiPIMS deposition (power equal to 300 W), the thinner sample (S7 and S10) show the higher conductivity compared to those of the thicker samples (S1 and S4) regardless of its at RT or 400°C deposition, as shown in Fig. 6(a). These measurement results are in good agreement with the theoretical resistivity calculation using Drude model (theoretical resistivity: S4 > S7), as shown in Table 3. When the thickness is < 50 nm, the density of the TiN films varies with different thickness, which results in optical and electric properties possess thickness-dependent properties, as shown in Fig. 6(b). The reason could be there is no major film stress gradient during the deposition procedure at a relatively thinner thickness < 50 nm [29]. A tendency for an increasing compressive stresses accompanied with an increasing in the defects [30]. Therefore, the electrical properties as well as the optical properties exhibit strongly thickness dependent when thickness is less than 50 nm. The damping frequency, which represents dissipation of the energy, of the above result shows the same trend as the smaller damping frequency for sample S7 (246.7 x 2π THz) than sample S4 (270.6 x 2π THz) in Table 3. Clearly, when the conductivity of TiN thin films is lower than 10^5 S/m, the optical properties also turn dielectric with a positive real part of the dielectric constant. It can be inferred from Fig. 7 that when the average power is less than 180 W, the XRD measurement shows amorphous characteristics, which corresponds to the dielectric-like samples. On the contrary, for the TiN thin films deposited at 300 W, the (111) orientation peak appears and there is a stronger diffraction signal at the (220) and (200) orientations, which represents better crystallinity with less grain boundaries. The grain sizes of (200) phase are 7.97 nm for sample S1, 7.46 nm for sample S2, and 5.69 nm for sample S3. Obviously, when reducing the sputtering power from 180 W to 80W, there would be a significantly reduction of the grain size accompanied with more grain boundaries which could cause more electron scattering losses, resulting in poor conductivity. Compared to the samples deposited at 80 W, the TiN thin films deposited at 300 W could have up to 25 times higher conductivity. Otherwise, from the results shown in Fig. 2, it can be seen that the HiPIMS sample has a higher plasma frequency compared to that of the DC sample but similar damping frequency. This result means that deposition with HiPIMS could further improve the crystallinity of TiN thin films during both RT and high-temperature deposition.

4.3 Optical properties and quality analysis: metal-like to dielectric-like behaviors

Among the metallic-like samples (S1, S2, S4, S5, S7, and S8), the wavelength of the transmittance peak (T_{peak}) is close to the wavelength of the reflectance dip (R_{dip}). On the contrary, the wavelength of the T_{peak} is not matched to the R_{dip} for the dielectric-like samples (S3, S6, and S9). For the dielectric-like samples, the significant shift of the T_{peak} and R_{dip} (> 50 nm) is due to the dielectric-like positive real part of the permittivity, which means there is no plasma frequency. The reflectance is mainly determined by thin-film interference. However, the spectral features of the metallic-like samples are due to the plasma frequency. Therefore,

Table 3. Drude model fitting of theoretical resistivity of TiN thin films with an average sputtering power of 300 W

Sample No.	Temperature: 400 °C		Sample No.	Temperature: RT		Sample No.	Temperature: RT	
	ω_p (x2π THz)	γ (x2π THz)		ω_p (x2π THz)	γ (x2π THz)		ω_p (x2π THz)	γ (x2π THz)
S1	1862	262.6	S4	1846	270.6	S7	1846	246.7
	$\frac{\gamma}{\omega_p^2} = 1.21\times10^{-17}$			$\frac{\gamma}{\omega_p^2} = 1.26\times10^{-17}$			$\frac{\gamma}{\omega_p^2} = 1.15\times10^{-17}$	

#245651 Received 14 Jul 2015; revised 14 Dec 2015; accepted 14 Jan 2016; published 20 Jan 2016
© 2016 OSA

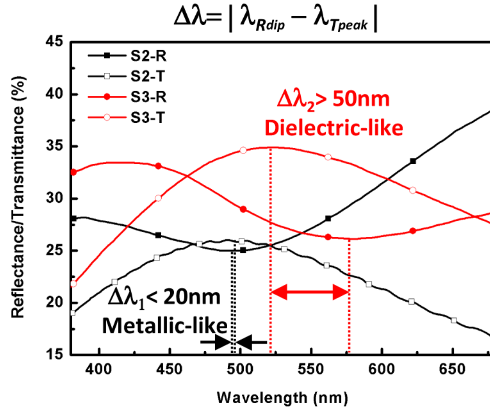

Fig. 8. Reflectance and transmittance spectra for metallic-like (S2) and dielectric-like (S3) TiN thin films deposited on B270 glass substrates in the wavelength region ranging from 380 nm to 680 nm. The reflectance spectra are indicated by the solid symbol and the transmittance spectra are indicated by the hollow symbol. For metallic-like samples (black), the reflectance dip and transmittance peak are close to each other. For the dielectric-like samples (red), there is a significant shift between the reflectance dip and transmittance peak.

Table 4. XRR measurements of TiN thin films deposited by DC magnetron sputtering and HiPIMS with different sputtering powers.

Sample	Temperature: 400 °C		Sample No.	Temperature: RT		Sample No.	Temperature: RT	
	Power (W)	Density (g/cm^3)		Power (W)	Density (g/cm^3)		Power (W)	Density (g/cm^3)
HiPIMS	300	5.25	S4	300	5.19	S7	300	5.30
			S5	180	5.00	S8	180	5.11
			S6	80	4.80	S9	80	4.86
DC	300	4.85	DC	300	4.70			

simple analysis of the reflectance and transmittance spectra could provide a good estimation of whether a TiN thin film has metallic-like or dielectric-like properties, as shown in Fig. 8. Low-angle X-ray reflectivity (XRR, PANalytical) measurements are used to determine the density of the TiN thin films. As can be seen in Table 4, among all the six samples using room temperature deposition, there is a trend that increasing sputtering power would result in higher density of TiN thin films. In addition, the sample with thickness = 23 nm (S7) is denser than the sample with thickness = 48 nm (S4), which corresponds well with the results shown in Table 3 that S7 has lower damping frequency than S4, because the denser film provides higher carrier mobility. If comparing to the DC magnetron sputtering, by using HiPIMS, the density obviously increases 8.2% at 400°C deposition (from 4.85 g/cm^3 to 5.25 g/cm^3). At room temperature, the density is with even stronger improvement of 10.5% (from 4.70 g/cm^3 to 5.19 g/cm^3). From the results, denser film could be realized by HiPIMS technique, which possesses less structural defects in the TiN thin films. The TiN thin films' root mean square roughness (R_q) were measured by atomic force microscopy under a tapping mode. Among all the samples, the roughness was found to be 1.5 nm to 3 nm, and there is no obvious trend in roughness with different sputtering powers. The ratio x of TiN_x thin films were obtained using X-ray photoelectron spectroscopy (XPS, Themo Fisher Scientific Theta Probe) with a Al Kα X-ray beam (monochromatic, energy = 1486.6 eV, beam size = 40 µm). The surface cleaning time by using Ar + sputtering is 50 second. From the XPS analysis, the composition of nitride tends to increase when the sample is fabricated using lower average power. (TiN_x, x = 1.04 for S4, x = 1.10 for S5, and x = 1.23 for S6), which means overstoichiometric TiN_x samples with higher composition in nitride would tend to function more like dielectrics.

#245651 Received 14 Jul 2015; revised 14 Dec 2015; accepted 14 Jan 2016; published 20 Jan 2016
© 2016 OSA

5. Conclusion

Magnetron sputtering has been widely used to fabricate alternative plasmonic materials, especially for transition metal nitrides. However, conventional DC magnetron sputtering faces restrictions in increasing the power to a very high level, due to limitations of the cooling system; high-power DC sputtering could damage the sputtering target, e.g. target melting and burn-through. By using the HiPIMS technique, the instantaneous bombardment energy to the target will increase by 2 to 3 orders of magnitude. Hence, TiN thin films with higher plasma frequencies or good thin-film quality could be realized by RT deposition. By using the HiPIMS technique with heating up to 400 °C, the crystallinity of TiN thin films could be further increased. In addition, TiN thin films fabricated by HiPIMS could possess higher conductivities with better uniformity, even for very thin TiN films with a thickness of 23 nm. Deposition with an average power greater than or equal to 180 W is needed to fabricate TiN thin films with metallic-like optical properties. TiN thin films with metallic properties have conductivities around 1×10^5 S/m to 7×10^5 S/m. On the other hand, for dielectric-like TiN thin films, interference dominates the observed spectral features, in which an obvious shift between T_{peak} and R_{dip} occurs.

In conclusion, TiN thin films with higher conductivity, less nitrogen vacancies, and a stable composition can be fabricated using the HiPIMS technique. In addition, good crystalline quality transition metal nitride (metallic-like) thin films deposited at RT are achieved, which is particularly important for the lift-off process with photoresist, or for deposition on flexible devices. Besides tuning the average power, controlling the on/off ratio of the HiPIMS system could also achieve effective momentum transfer to the deposited thin films. TiN-based plasmonics and metamaterials can be fabricated by HiPIMS. TiN thin films with tunable plasma frequency can be used in future applications, like refractory metamaterial absorbers.

Acknowledgments

This work is supported by The Ministry of Science and Technology, Taiwan, ROC (Project No. 103-2221-E-009-067). Special thanks for the technical support from Nancy Chu in Instrument Technology Research Center, sample fabrication from Mao-Guo Sum, and AFM measurements from Yu-Lun Kuo and Zu-Wen Xie.

#245651 Received 14 Jul 2015; revised 14 Dec 2015; accepted 14 Jan 2016; published 20 Jan 2016
© 2016 OSA